



**HAL**  
open science

## **NTRK -rearranged spindle cell neoplasms are ubiquitous tumours of myofibroblastic lineage with a distinct methylation class**

Arnault Tauziède-espariat, Mathilde Duchesne, Jessica Baud, Mégane Le Quang, Dorian Bochaton, Rihab Azmani, Sabrina Croce, Isabelle Hostein, Carole Kesrouani, Delphine Guillemot, et al.

### ► To cite this version:

Arnault Tauziède-espariat, Mathilde Duchesne, Jessica Baud, Mégane Le Quang, Dorian Bochaton, et al.. NTRK -rearranged spindle cell neoplasms are ubiquitous tumours of myofibroblastic lineage with a distinct methylation class. *Histopathology*, 2022, 82, pp.596 - 607. 10.1111/his.14842 . hal-04094724

**HAL Id: hal-04094724**




**<https://u-paris.hal.science/hal-04094724>**

Submitted on 11 May 2023

**HAL** is a multi-disciplinary open access archive for the deposit and dissemination of scientific research documents, whether they are published or not. The documents may come from teaching and research institutions in France or abroad, or from public or private research centers.

L'archive ouverte pluridisciplinaire **HAL**, est destinée au dépôt et à la diffusion de documents scientifiques de niveau recherche, publiés ou non, émanant des établissements d'enseignement et de recherche français ou étrangers, des laboratoires publics ou privés.

# NTRK-rearranged spindle cell neoplasms are ubiquitous tumours of myofibroblastic lineage with a distinct methylation class

Arnault Tauziède-Espariat,<sup>1,2</sup>  Mathilde Duchesne,<sup>3</sup> Jessica Baud,<sup>4</sup> Mégane Le Quang,<sup>4,5</sup> Dorian Bochaton,<sup>6</sup> Rihab Azmani,<sup>7</sup> Sabrina Croce,<sup>4</sup> Isabelle Hostein,<sup>4</sup> Carole Kesrouani,<sup>8</sup> Delphine Guillemot,<sup>6</sup> Gaëlle Pierron,<sup>6,9</sup> Franck Bourdeaut,<sup>10,11</sup> Liesbeth Cardoen,<sup>12</sup>  Lauren Hasty,<sup>1</sup> Emmanuèle Lechapt,<sup>1</sup> Alice Métails,<sup>1</sup> Fabrice Chrétien,<sup>1</sup> Stéphanie Puget,<sup>13</sup> Pascale Varlet<sup>1,2</sup> & François Le Loarer<sup>3,5,14</sup> 

<sup>1</sup>Department of Neuropathology, GHU Paris –Psychiatry and Neuroscience, Sainte-Anne Hospital, <sup>2</sup>Université de Paris, INSERM, U1266, Institute of Psychiatry and Neurosciences of Paris (IPNP), Paris, <sup>3</sup>Department of Pathology, Dupuytren University Hospital, Limoges, <sup>4</sup>Department of Biopathology, Institut Bergonié, Bordeaux, <sup>5</sup>Université de Bordeaux, Talence, <sup>6</sup>Laboratory of Somatic Genetics, Institut Curie Hospital, Paris, <sup>7</sup>Department of Bioinformatics, Institut Bergonié, Bordeaux, France, <sup>8</sup>Department of Pathology, Faculty of Medicine, Saint Joseph University of Beirut, Beirut, Lebanon, <sup>9</sup>Paris-Sciences-Lettres, Institut Curie Research Center, INSERM, U830, <sup>10</sup>SIREDO Center Care, Innovation, Research in Pediatric, Adolescent and Young Adult Oncology, Curie Institute and Paris Descartes University, <sup>11</sup>Université de Paris, <sup>12</sup>Department of Radiology, Curie Institute, Paris University, <sup>13</sup>Department of Paediatric Neurosurgery, Necker Hospital, APHP, Université Paris Descartes, Sorbonne Paris Cité, Paris and <sup>14</sup>INSERM U1218, ACTION, Institut Bergonié, Bordeaux, France

Date of submission 29 July 2022

Accepted for publication 17 September 2022

Published online Article Accepted 22 November 2022

Tauziède-Espariat A, Duchesne M, Baud J, Le Quang M, Bochaton D, Azmani R, Croce S, Hostein I, Kesrouani C, Guillemot D, Pierron G, Bourdeaut F, Cardoen L, Hasty L, Lechapt E, Métails A, Chrétien F, Puget S, Varlet P & Le Loarer F

(2023) *Histopathology* 82, 596–607. <https://doi.org/10.1111/his.14842>

## NTRK-rearranged spindle cell neoplasms are ubiquitous tumours of myofibroblastic lineage with a distinct methylation class

**Aims:** *NTRK* gene fusions have been described in a wide variety of central nervous system (CNS) and soft tissue tumours, including the provisional tumour type ‘spindle cell neoplasm, *NTRK*-rearranged’ (SCN–*NTRK*), added to the 2020 World Health Organisation Classification of Soft Tissue Tumours. Because of histopathological and molecular overlaps with other soft tissue entities, controversy remains concerning the lineage and terminology of SCN–*NTRK*.

**Methods and results:** This study included 16 mesenchymal tumours displaying kinase gene fusions (*NTRK* fusions and one *MET* fusion) initially diagnosed as infantile fibrosarcomas (IFS), SCN–*NTRK* and adult-

type fibrosarcomas from the soft tissue, viscera and CNS. We used immunohistochemistry, DNA methylation profiling, whole RNA-sequencing and ultrastructural analysis to characterise them. Unsupervised *t*-distributed stochastic neighbour embedding analysis showed that 11 cases (two CNS tumours and nine extra-CNS) formed a unique and new methylation cluster, while all tumours but one, initially diagnosed as IFS, clustered in a distinct methylation class. All the tumours except one formed a single cluster within the hierarchical clustering of whole RNA-sequencing data. Tumours from the novel methylation class co-expressed CD34 and S100, had variable histopathological grades and frequently displayed a *CDKN2A* deletion. Ultrastructural analyses evidenced a myofibroblastic differentiation.

**Conclusions:** Our findings confirm that SCN–*NTRK* share similar features in adults and children and in

Address for correspondence: A. Tauziède-Espariat, Department of Neuropathology, GHU Paris-Psychiatrie et Neurosciences, Sainte-Anne Hospital, 1 rue Cabanis, 75014 Paris, France.  
e-mail: a.tauziede-espariat@ghu-paris.fr

all locations combine an infiltrative pattern, distinct epigenetic and transcriptomic profiles, and ultrastructural evidence of a myofibroblastic lineage. Further

studies may support the use of new terminology to better describe their myofibroblastic nature.

Keywords: central nervous system, DNA methylation profile, myofibroblastic, NTRK, soft tissue

## Introduction

*NTRK1/2/3* gene fusions are involved in a wide variety of tumour types in different organs.<sup>1</sup> There is a striking diversity in soft tissue, as *NTRK* fusions have been reported in inflammatory myofibroblastic tumours (IMT),<sup>2</sup> infantile fibrosarcomas (IFS)<sup>3</sup> and the 'spindle cell neoplasm with *NTRK* fusion' (SCN–*NTRK*).<sup>4</sup> This provisional category, included in the 2020 World Health Organisation (WHO) Classification of Soft Tissue Tumours, is associated with a wide morphological spectrum [IFS, IMT, lipofibromatosis-like neural tumour and malignant peripheral nerve sheath tumour (MPNST)].<sup>4</sup> SCN–*NTRK* harbour mainly *NTRK1/2/3* gene fusions (75 reported cases to date).<sup>5–17</sup> Alternative fusions (implicating *ALK*, *BRAF*, *MET*, *RAF1*, *RET* and *ROS1* genes) have also been reported, and their exact relationship to SCN–*NTRK* remains unknown.<sup>8,19–27</sup> The histological lineage of these ubiquitous tumours [mainly located in soft tissue, but also in viscera and even in the central nervous system (CNS)] has not been elucidated to date.<sup>11,20</sup> While the WHO Classification of soft tissue tumours has classified them within tumours of uncertain differentiation, SCN–*NTRK* were listed within the myofibroblastic/fibroblastic category in the 2022 WHO classification of paediatric tumours.<sup>26,27</sup> Recently, the 2021 WHO classification of CNS tumours has been enriched with a wide variety of new tumour types identified thanks to DNA-methylation profiling,<sup>28–30</sup> representing a combination of both somatically acquired DNA methylation changes and a signature reflecting the cell of origin.<sup>31,32</sup> A DNA-methylation based classifier has been created for sarcomas but does not yet cover SCN–*NTRK*.<sup>33</sup> To identify the lineage of SCN–*NTRK* and further characterise their histopathological/molecular features, we analysed a cohort of *NTRK*-fused mesenchymal tumours using histopathology, ultrastructural analyses, whole RNA-sequencing and DNA-methylation profiling.

## Materials and methods

### SAMPLE COLLECTION AND CLINICAL DATA

Tumour samples were provided by the consultation archive database (1982–2021) from the Department

of Neuropathology at Sainte-Anne Hospital, NetSarc+ and Institut Bergonie. Fifteen mesenchymal tumours with a proven *NTRK* fusion were selected for this study. Additionally, one CNS case suspected to be SCN–*NTRK* harbouring a *TFG::MET* fusion was also included. Patient characteristics and clinical data were retrieved from hospital records and included sex, age at presentation and medical history.

Parents/guardians gave written informed consent for the retrospective analysis of clinical data according to the Institutional Review Board and before inclusion into ongoing protocols. All soft tissue cases are recorded in the database of the French expert sarcoma network (RRePS/Netsarc+), which is approved by the National Committee for Protection of Personal Data (CNIL, no. 910390). The study was also approved by the research board of Institut Bergonie. The analyses of tissue were performed in accordance with local ethics regulations. Parents/guardians gave written informed consent for the retrospective analysis of clinical data according to the Institutional Review Board and before inclusion into ongoing protocols. The data supporting the findings of this study are available from the corresponding author upon reasonable request.

### HISTOPATHOLOGICAL REVIEW AND IMMUNOHISTOCHEMISTRY

The central pathology review was performed jointly by two neuropathologists (ATE and PV) and soft tissue pathologists (FLL, MLQ). A representative paraffin block was selected for each case. Unstained 3- $\mu$ m-thick slides of formalin-fixed, paraffin-embedded (FFPE) tissues were obtained and submitted for immunostaining (the list of antibodies is detailed in Supporting information, Table S1). External positive and negative controls were used for all antibodies.

### WHOLE RNA-SEQUENCING AND BIOINFORMATIC ANALYSIS

Total RNA was extracted from the FFPE blocks and library prepared using the TruSeq RNA Access Library Prep Kit (Illumina, San Diego, CA, USA) and

sequenced with an Illumina NextSeq 500 automat (Illumina), as previously described.<sup>34</sup> Gene expression was measured using counts of sequencing reads with the software HtSeq version 0.6.0.<sup>35</sup> Gene count data were normalised using the VOOM method.<sup>36</sup> Unsupervised clustering was performed using agglomerative hierarchical clustering with distance criteria (1-Pearson\_correlation) and linkage criteria using the function hclust available in R.<sup>37</sup> Consensus clustering was performed with the package ConsensusClusteringPlus from BioConductor.<sup>38</sup> The fusion and cluster analyses were performed as previously described.<sup>34</sup> To achieve clustering, we used a set of control samples that encompassed similar histotypes to those included in the methylation analysis: undifferentiated pleomorphic sarcomas ( $n = 12$ ), MPNST (four), atypical neurofibromatous neoplasms of uncertain biological potential (two), meningiomas (five), dermatofibrosarcoma protuberans (nine), infantile hemispheric glioma with *BRAF* fusion (one), IFS (one), solitary fibrous tumour (SFT) (three), low-grade fibromyxoid sarcomas (four), fibromatosis with *CTNNB1* mutations (seven) and angiomatoid fibrous histiocytomas (AFH) (four) (Supporting information, Table S1).

#### DNA METHYLATION ARRAY PROCESSING AND COPY NUMBER PROFILING

Genomic DNA was extracted from fresh-frozen or FFPE tissue samples. DNA methylation profiling for all samples was performed using the Infinium MethylationEPIC (850 k) BeadChip (Illumina) or Infinium HumanMethylation450 (450 k) BeadChip array (Illumina), as previously described.<sup>28</sup> The resulting matrix was used as input for a *t*-SNE analysis (*t*-distributed stochastic neighbour embedding; Rtsne package version 0.15) with a perplexity set to 10, maximum iteration to 500, resulting in two more easily interpretable dimensions (using a control set of 241 well-characterised reference tumours representing a wide variety of tumour types from the Brain Tumour and Sarcoma Classifiers of Heidelberg).<sup>28,33</sup>

#### ULTRASTRUCTURAL ANALYSES

A representative section was first selected for each case from FFPE tissues stained with haematoxylin phloxin saffron (HPS). Then, tissues were deparaffinised and fixed for 1 h in glutaraldehyde. After the dehydration processing, the tissues were embedded in Epon. Semi-thin sections (1- $\mu$ m-thick slides) were stained with toluidine blue. Ultrathin sections (90 nm) were stained with lead citrate and uranyl acetate, then

observed under an electronic microscope (JEOL JEM 1400 Flash). Analysis was performed at the Pathology Department of Limoges University Hospital by one neuropathologist (MD).

## Results

### HISTOPATHOLOGICAL FINDINGS

Histopathological results are detailed in Supporting information, Table S1. Considering the age of patients, the central histopathological review classified the 16 tumours as SCN–NTRK ( $n = 8$ ), IFS ( $n = 5$ ) and adult-type fibrosarcomas ( $n = 3$ ). SCN–NTRK were highly infiltrative, whatever the organ concerned (Figure 1A,B). The tumours were composed of spindle cells arranged in intersecting fascicles, with a variable cellular density (low to high, Figure 1C,D and Supporting information, Table S1). The tumour cells presented a pale scant cytoplasm with indistinct cell borders and fusiform nuclei with inconspicuous nucleoli (Figure 1C,D). Focally, we observed nuclear atypia with hyperchromasia and pleomorphism and an elevated mitotic index (up to 37 mitoses per 1.7 mm<sup>2</sup>) in some cases (Figure 1E). Necrosis was only observed in one recurrent case (Figure 1F). All cases presented areas of fibrous stroma and five of eight (62%) exhibited a perivascular hyalinisation forming collagen rings (Figure 1G). A myxoid stroma was present in four of eight cases (50%). Three cases (37%) presented inflammatory infiltrates composed as foci of lymphocytes and plasma cells. Immunohistochemical analysis showed that all tumours co-expressed S100 and CD34 (Figure 1H,I), ranging from focal to diffuse staining. Smooth muscle actin was only focally expressed in two of eight cases (25%). SOX10 was not expressed. The proliferation index (Ki67) ranged from 1 to 50%, with a median of 2.5%. For one case (case 16), paired samples of the first surgery and the recurrence were available (see below for details): the first tumour presented a low cellular density, without necrosis and low mitotic and proliferative indexes, whereas the recurrence exhibited signs of malignancy (necrosis, elevated mitotic and proliferative indices and anisokaryosis).

All IFS cases affected infants (all aged less than 1 year) and displayed a fascicular architecture. Tumour cells harboured monotonous medium-sized nuclei with clear chromatin along with a pale eosinophilic cytoplasm. The accompanying stroma was limited to small fibrous foci in all cases. Large dilated vessels with haemorrhage were seen in three cases



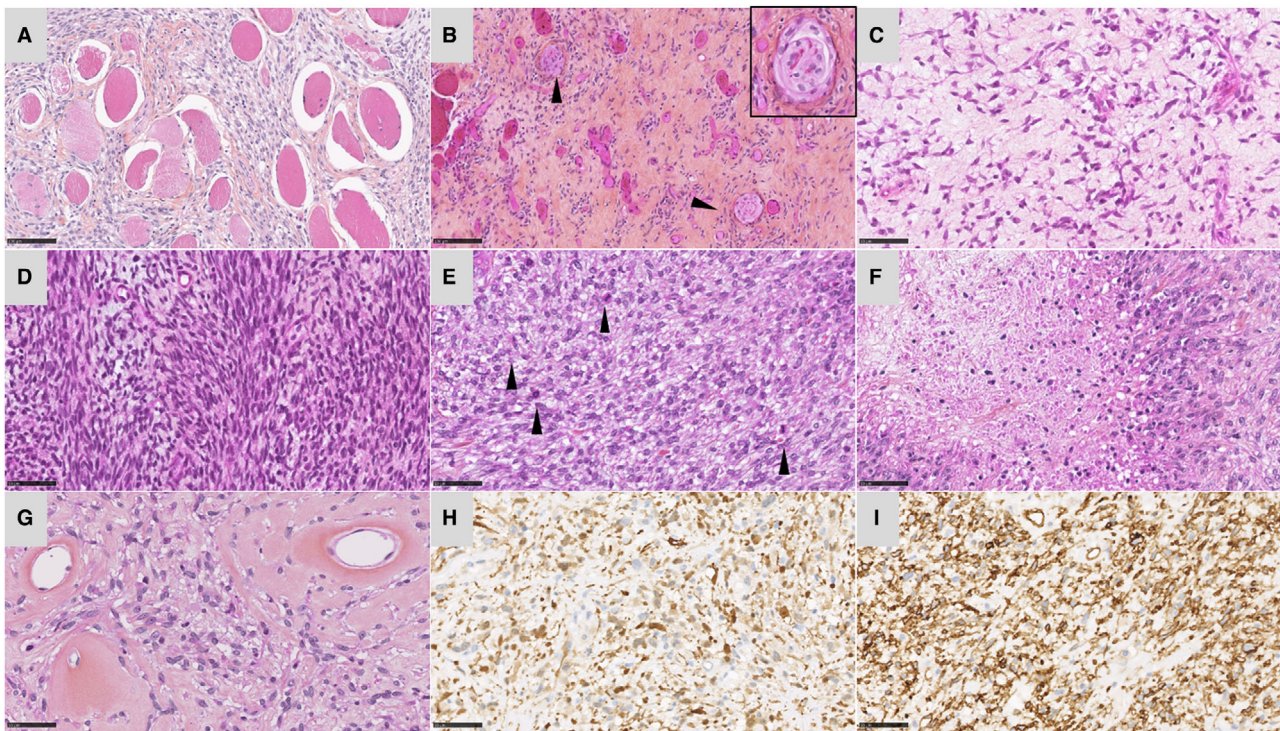


**Figure 1.** Histopathological and ultrastructural features of tumours from the new methylation class. (A) Infiltration of skeletal muscle by tumour cells (case 13, HPS). (B) Meningothelial cells (arrowheads) included in the proliferation (case 1, HPS). (C) Spindle cell proliferation associated with an abundant myxoid stroma (case 1, HPS). (D) Another area showing tumour cells densely arranged in fascicles (case 1, HPS). (E) Cellular proliferation of spindle and epithelioid cells showing a brisk mitotic activity (arrowheads) (case 16, HPS). (F) Area of necrosis (case 16). (G) Perivascular collagen rings (case 1). (H) Strong expression of S100 (case 16). (I) Diffuse expression of CD34 (case 16). Scale bars represent 100  $\mu$ m (A,B) and 50  $\mu$ m (C–I). HPS, haematoxylin phloxin saffron.

(three of five). Tumours expressed CD34 in one of four cases.

Adult-type fibrosarcomas affected adults with a mean age of 55 years (ages ranged from 48 to 66 years). All cases displayed a fascicular architecture. Tumour cells were arranged in densely cellular fascicles. Large vessels with haemorrhage were present in all cases. Tumour cells harboured ovoid nuclei and a majority of nuclei were monotonous, but anisokaryosis was also present focally in all cases taking the form of hyperchromatism and/or larger multilobulated nuclei. The stroma was heterogeneous and absent in some areas or collagenous in some foci. The mean mitotic index was 10/10 high-power fields.

#### WHOLE RNA-SEQUENCING FINDINGS

In eight cases, *NTRK1* was fused with the following 5' partners: *TPM3* (four of eight), *IRF2BP2* (two of eight) and *LMNA* and *TPR* (one case each). *NTRK3* was only found fused in 5' with *ETV6* (seven of seven). One case was associated with a *TFG::MET*

fusion. Unsupervised RNA-sequencing cluster analysis showed that 15 of the 16 cases clustered together, independently of their location and their histopathological subtype (Figure 2). Based on this clustering, these 15 cases were subdivided into three subgroups: one of four tumours clustering with IFS; two of two tumours with a *TPM3::NTRK1* fusion and three of nine tumours harbouring *NTRK1/3* fusions (eight) and the case *MET*-fused. The last case (no. 15), presenting an *ETV6::NTRK3* fusion, segregated with an *ALK*-fused IMT (Figure 2).

#### DNA METHYLATION FINDINGS

Using DNA methylation-based brain tumour and sarcoma classifiers (latest versions: 12.5/12.2, which include more than 96 000 samples), nine of 16 were significantly classified (calibrated scores for DNA methylation class  $\geq 0.9$ ) as sarcoma (MPNST-like) (six) and IFS (three). Then, on *t*-SNE analysis performed in order to visualise actual distances and similarities between the different tumours, our cohort

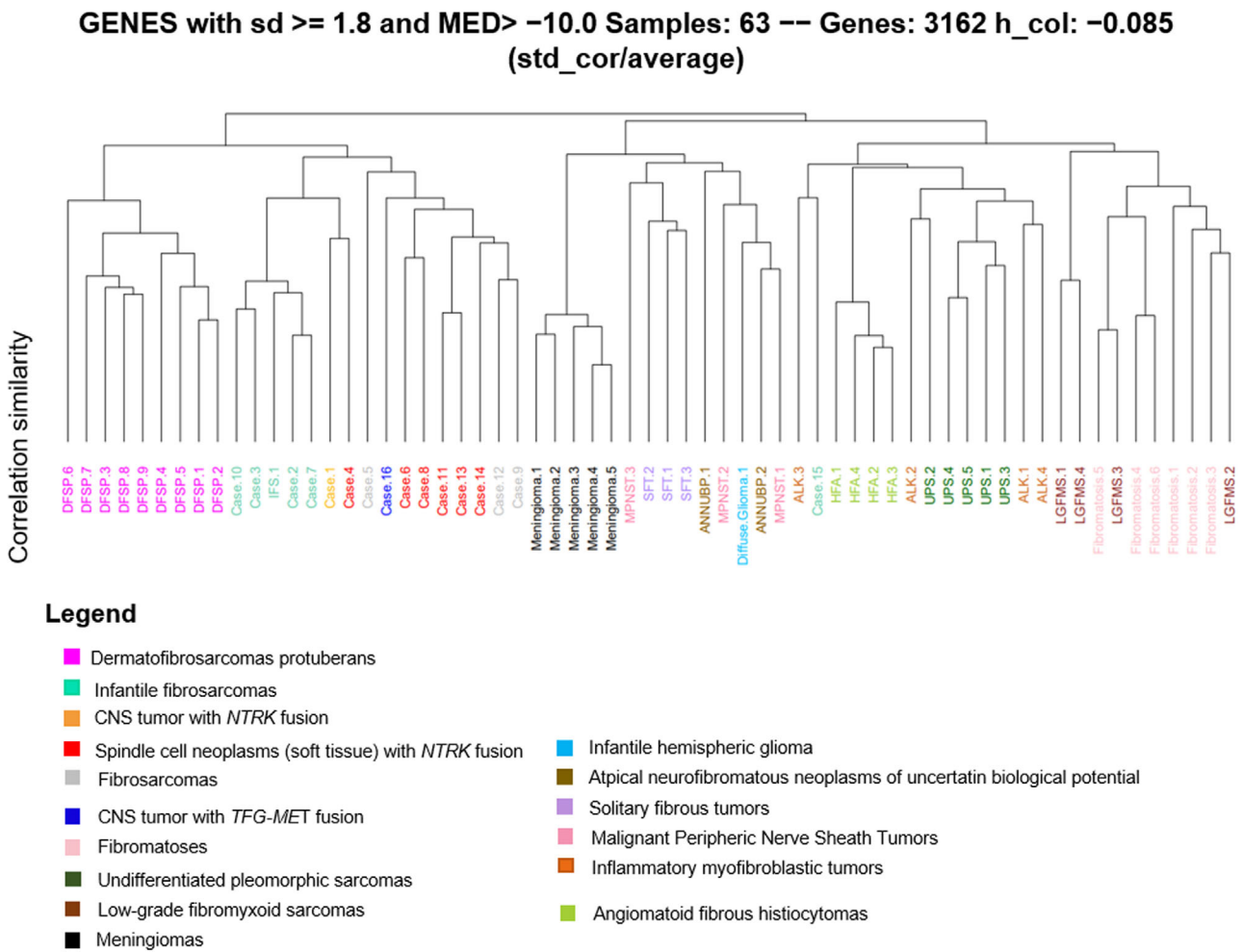


**Figure 2.** Unsupervised RNA-sequencing clustering analysis. The control cohort included: *ALK*-fused inflammatory myofibroblastic tumours (IMT), angiomatoid fibrous histiocytomas (AFH), desmoid-type fibromatosis, undifferentiated pleomorphic sarcomas (UPS), dermatofibrosarcoma protuberans (DFSP), low-grade fibromyxoid sarcomas (LGFMS), meningiomas, solitary fibrous tumours (SFT), malignant peripheral nerve sheath tumours (MPNST) and atypical neurofibromatous neoplasms of uncertain biological potential (ANNUBP).

segregated into three different groups (Figure 3A). The largest fraction (11 of 16, 69%) of tumours formed a novel cluster clearly distinct from the reference entities. Four tumours (four of 16, 25%) were classified within the IFS cluster. The last tumour (case 15) was classified among AFH (one of 16, 6%). In light of the copy number data, we identified a *CDKN2A* deletion in six of 11 (55%) tumours belonging the new methylation class (MC). Interestingly, no other tumour from our cohort presented this alteration. This deletion was confirmed by a FISH (fluorescence *in-situ* hybridisation) analysis of the *CDKN2A* locus showing a homozygous deletion (Figure 3B). No *NF1* deletion was seen (none of 16).

#### INTEGRATED DIAGNOSES

Accordingly, eight cases, which included adult cases and one infant (cases 1, 4, 6, 8, 11, 13, 14 and 16), were classified as SCN–NTRK by histopathology and clustered together using DNA-methylation profiling and RNA-sequencing. They presented as infiltrative spindle cells with a coexpression of S100 protein and CD34 and harboured *NTRK1* (seven) or a *MET* (one) fusion. Accordingly, four cases, all infants (cases 2, 3, 7 and 10) were classified as IFS by histopathology and clustered together using DNA-methylation profiling and RNA-sequencing. They presented typical histopathological features of IFS and harboured the classical *ETV6::NTRK3* fusion. The three cases (cases

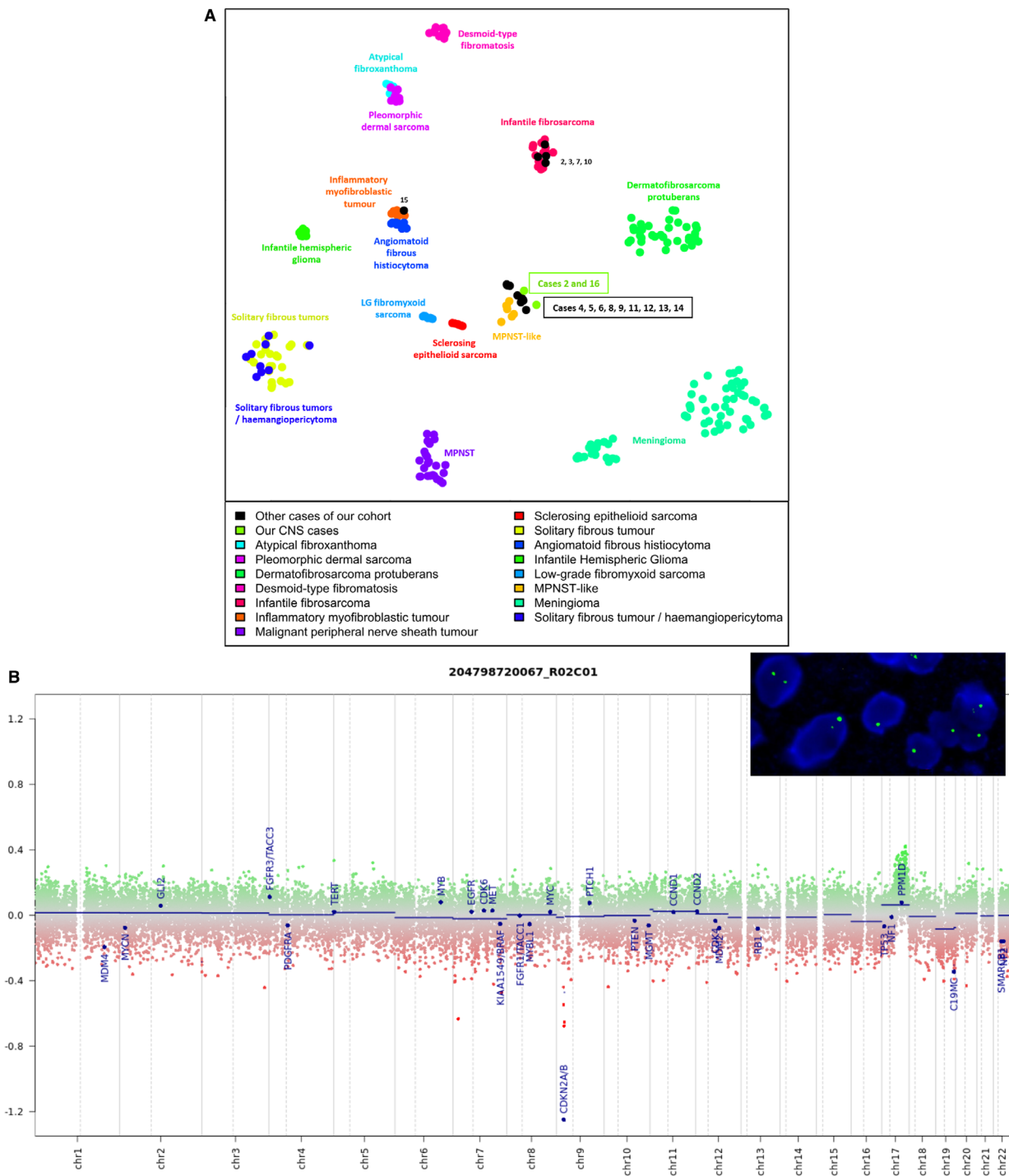


**Figure 3.** Epigenetic and copy number variation features. (A) *t*-Distributed stochastic neighbour embedding (*t*-SNE) analysis of DNA methylation profiles from the 16 investigated tumours alongside selected reference samples. Reference DNA methylation diagnoses: five angiomatoid fibrous histiocytomas, five atypical fibroxanthomas, 36 dermatofibrosarcomas protuberans, 13 desmoid-type fibromatoses, 14 infantile fibrosarcomas, nine infantile hemispheric gliomas, seven inflammatory myofibroblastic tumours, eight low-grade fibromyxoid sarcomas, 25 malignant peripheral nerve sheath tumours, 67 meningiomas, seven MPNST-like, nine pleomorphic dermal sarcomas, six sclerosing epithelioid sarcomas, 26 solitary fibrous tumours, nine solitary fibrous tumours/haemangiopericytomas. (B) Illustrative copy number variation of case 1 showing a 9p deletion confirmed by FISH analysis of *CDKN2A* locus showing a homozygous deletion (no orange signal with green signals representing the control centromeric of the chromosome 9). FISH, fluorescence *in-situ* hybridisation.



5, 9 and 12) initially diagnosed as adult-type fibrosarcomas clustered with the subgroup of SCN–NTRK by DNA-methylation profiling and RNA-sequencing despite histopathological features of malignancy. They presented coexpression of S100 and CD34, and were associated with *NTRK3* (two) and *NTRK1* (one) fusions. The last case (case 15) concerned an infantile tumour classified as IFS by histopathology with the classical *ETV6::NTRK3* fusion, but clustered with AFH (by RNA-sequencing) and IMT (by DNA-methylation profiling). Based on the WHO classification and because of discrepancies between histopathology, transcriptomic and epigenetic results, no integrated diagnosis was made.

#### ULTRASTRUCTURAL FINDINGS

Ultrastructural analyses were interpretable in 11 cases (Supporting information, Table S1). All tumours, including those from the new MC, harboured features suggestive of a myofibroblastic differentiation; namely, indentation of nuclei (Figure 4A), presence of abundant myofilament bundles with core densities within the cytoplasm (Figure 4B), either with a

subplasmalemmal location or loosely arranged in the cytoplasm, and the rough endoplasmic reticulum (Figure 4A,C). However, their exact location could not be determined due to artefacts related to the FFPE pre-analytical conditions of the samples. Finally, extracellular collagen was present in the matrix (Figure 4D).

#### CORRELATION WITH CLINICAL DATA AND PATIENTS' OUTCOME

The patients' clinical data are summarised in Table 1. Tumour locations of the new MC were ubiquitous, including the following anatomical sites: soft tissue (six), viscera (three) and CNS (two). The median age at diagnosis was 30.5 years (ranging from 1 to 66) with a female predominance (82%, nine of 11). Outcome data were available for nine of 11 patients (median follow-up of 21 months); two died of their disease (24 and 49 months after the initial diagnosis). Interestingly, one case (case 16) associated with a *TFG::MET* fusion had initially benefited from a targeted therapy with crizotinib, until drug toxicity led to the interruption of the treatment (Figure 5). Despite other treatments, the subsequent imaging

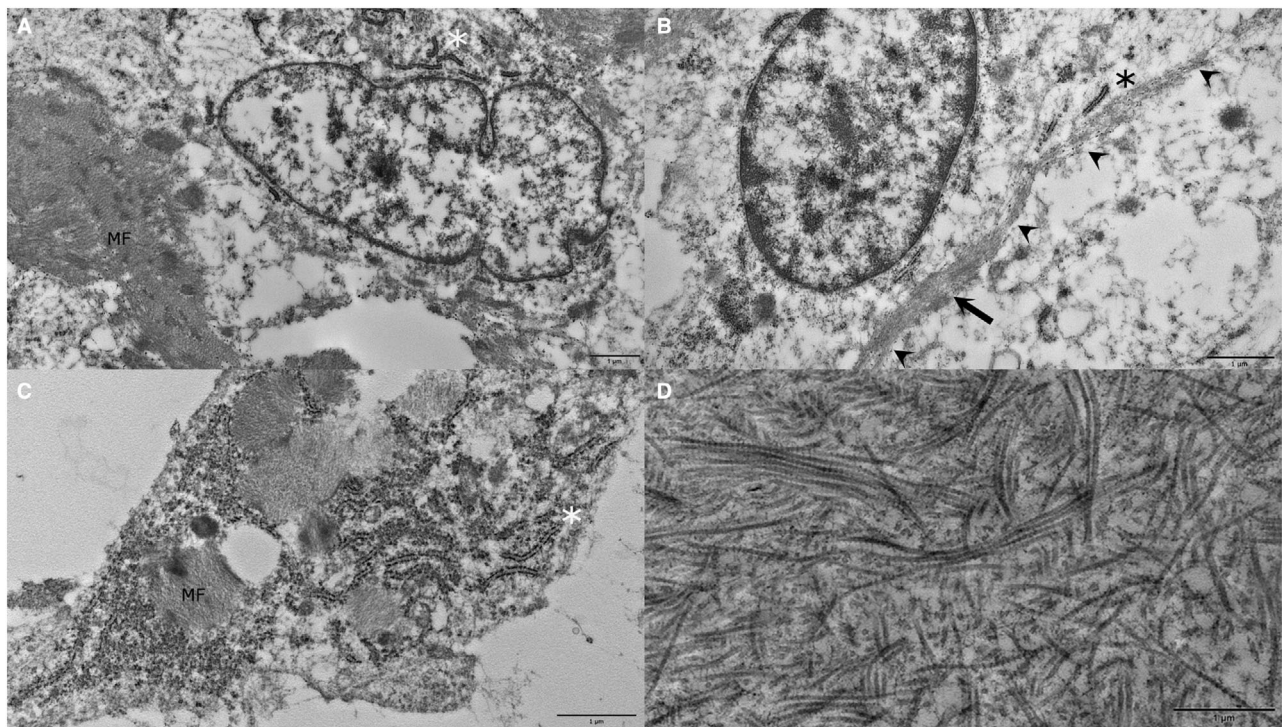


**Figure 4.** Ultrastructural features of tumours from the new methylation class. (A) Presence of indented nucleus, intracytoplasmic myofilaments with core densities (MF) and rough endoplasmic reticulum (\*) in tumour cells. (B) Presence of rough endoplasmic reticulum (\*) and intracytoplasmic subplasmalemmal bundles of myofilaments (arrow) whose plasma membrane can be estimated (arrowheads). (C) Intracytoplasmic myofilaments with core densities (MF) and rough endoplasmic reticulum (\*) in tumour cells. (D) Presence of collagen fibres.



**Table 1.** Clinical and molecular data of cases from our cohort

Case	Sex	Age (years)	Histological diagnosis	Location	Fusion transcript/RNA-sequencing cluster	DNA methylation classification with the sarcoma classifier v12.2 version (calibrated score)	t-SNE analysis methylation cluster	Chr. 9p status	FO
2	M	0	Infantile fibrosarcoma	Chest wall (soft tissue)	ETV6(ex5)-NTRK3(ex15)/infantile fibrosarcoma	Infantile fibrosarcoma (0.99)	Infantile fibrosarcoma	Balanced	ANED (84 months)
3	M	0	Infantile fibrosarcoma	Presacral (soft tissue)	ETV6(ex5)-NTRK3(ex14)/infantile fibrosarcoma	Infantile fibrosarcoma (0.99)	Infantile fibrosarcoma	Balanced	ANED (14 months)
7	F	1	Infantile fibrosarcoma	Paravertebral (soft tissue)	ETV6(ex5)-NTRK3(ex15)/infantile fibrosarcoma	Infantile fibrosarcoma (0.99)	Infantile fibrosarcoma	Balanced	NA
10	F	0	Infantile fibrosarcoma	Pelvis (soft tissue)	ETV6(ex5)-NTRK3(ex15)/infantile fibrosarcoma	Infantile fibrosarcoma (0.85)	Infantile fibrosarcoma	Balanced	ANED (65 months)
1	M	17	Spindle cell neoplasm with NTRK fusion	Brain	TPM3(ex7)-NTRK1(ex12)/new cluster	Sarcoma (MPNST-like) (0.72)	New methylation class	Balanced	AWD (13 months)
4	F	29	Spindle cell neoplasm with NTRK fusion	Uterus	TPM3(e3)-NTRK1(e10)/new cluster	Sarcoma (MPNST-like) (0.99)	New methylation class	Balanced	ANED (11 months)
5	F	48	Adult type fibrosarcoma	Pancreas	ETV6(ex4)-NTRK3(ex13)/new cluster	Infantile fibrosarcoma (0.39)	New methylation class	Deleted	ANED (12 months)
6	F	56	Spindle cell neoplasm with NTRK fusion	Finger (cutaneous)	TPM3(ex9,7,8)-NTRK1(ex9,10)/new cluster	Sarcoma (MPNST-like) (0.99)	New methylation class	Balanced	ANED (21 months)
8	F	36	Spindle cell neoplasm with NTRK fusion	Foot sole (cutaneous)	TPR(ex21)-NTRK1(ex3,2)/new cluster	Sarcoma (MPNST-like) (0.26)	New methylation class	Balanced	ANED (50 months)
9	F	66	Adult type fibrosarcoma	Ankle (cutaneous)	IRF2BP2(ex2)-NTRK1(ex9,10)/new cluster	Sarcoma (MPNST-like) (0.99)	New methylation class	Deleted	DOD (24 months)
11	M	27	Spindle cell neoplasm with NTRK fusion	Neck (fascia)	TPM3(ex8,7)-NTRK1(ex9,10)/new cluster	Sarcoma (MPNST-like) (0.90)	New methylation class	Balanced	ANED (34 months)
12	F	50	Adult type fibrosarcoma	Stomach	ETV6(ex4)-NTRK3(ex13)/new cluster	Sarcoma (MPNST-like) (0.81)	New methylation class	Deleted	AWD (12 months)

**Table 1.** (Continued)

Case	Sex	Age (years)	Histological diagnosis	Location	Fusion transcript/RNA-sequencing cluster	DNA methylation classification with the sarcoma classifier v12.2 version (calibrated score)	t-SNE analysis methylation cluster	Chr. 9p status	FO
13	F	32	Spindle cell neoplasm with NTRK fusion	Palm (soft tissue)	IRF2BP2(ex1)-NTRK1(ex9)/new cluster	Sarcoma (MPNST-like) (0.99)	New methylation class	Deleted	NA
14	F	21	Spindle cell neoplasm with NTRK fusion	Thorax (soft tissue)	LMNA(ex2)-NTRK1(ex11)/new cluster	Sarcoma (MPNST-like) (0.95)	New methylation class	Deleted	NA
16	F	1	Spindle cell neoplasm with NTRK fusion	Meninge	TFG(ex4)-MET (ex15) /new cluster	Dermatofibrosarcoma protuberans (0.83)	New methylation class	Deleted	DOD (49 months)
15	F	1	Infantile fibrosarcoma	Axillary region (soft tissue)	ETV6(ex5)-NTRK3(ex14)/angiomatoid fibrous histiocytoma	Angiomatoid fibrous histiocytoma (0.74)	Inflammatory myofibroblastic tumour	Balanced	ANED (108 months)

ANED, Alive with no evidence of disease; AWD, Alive with disease; Chr., Chromosome; DOD, Died of disease; F, Female; FO, Follow-up; M, Male; MPNST, Malignant peripheral nerve sheath tumour; *t*-SNE, *t*-distributed stochastic neighbour embedding; NA, Not applicable.

revealed a local and metastatic progression, and the patient died 49 months after the initial diagnosis.

## Discussion

As per the last WHO classification of soft tissue tumours, the lineage of SCN–NTRK remains unknown. Because of their S100 immunoreactivity and spindle cell pattern, a potential neural differentiation was initially suggested.<sup>5,6,8,10,13–15,21,22,39</sup> In this study, we show that SCN–NTRK share a common DNA-methylation profile known to be correlated with a distinct cell of origin. According to *t*-SNE analysis, they were distinct from ‘MPNST-like sarcomas’. ‘MPNST-like sarcomas’ have only been described in the DNA-methylation classifier under DKFZ (as para-spinal tumours occurring in adults aged 50 years, with *NF1* alteration and no *NTRK* fusion, but retained H3K27me3) and are different from *NTRK*-fused tumours.<sup>40</sup> Our results are in line with the literature data suggesting a fibroblastic/myofibroblastic differentiation in SCN–NTRK.<sup>41–43</sup> Presence of intercellular collagen and rough endoplasmic reticulum and actin myofilaments were observed in the subplasmalemmal area (in a minority of cases) or arranged in a more

loosely attributed pattern (possibly due to the pre-analytical conditions of FFPE samples and because those tumours may not necessarily retain the characteristics of a mature non-tumoral myofibroblast).<sup>41,42</sup> Similarly to other myofibroblastic tumours,<sup>27,43–47</sup> myogenic markers (particularly smooth muscle actin and desmin) are heterogeneously expressed in SCN–NTRK.<sup>6,9–11,13–15,18,20,21,23,25</sup> SCN–NTRK may be confused with other entities due to the diversity of morphologies. Infantile forms of SCN–NTRK (20% of reported cases<sup>6,9–11,17,20–22</sup>) may share histopathological and genetic features (*ETV6::NTRK3* fusion, as in two current cases, or *ALK* fusions<sup>5,22</sup>) with IFS and IMT. Reciprocally, few cases of IFS and IMT have been reported with *NTRK* fusions.<sup>48–51</sup> Herein, SCN–NTRK form a MC clearly distinct from IMT and IFS, showing the interest of DNA-methylation profiling in difficult cases. However, a grey zone emerges with one case from our series (case 15) presenting histopathologically and genetically (*ETV6::NTRK3* fusion) as an IFS, but did not classify within this MC or as SCN–NTRK when analysed by DNA-methylation profiling. This case was classified as an AFH, despite being clinically and morphologically typical of IFS and despite harbouring the typical *ETV6::NTRK3* fusion of IFS. This result could not be explained and illustrates the

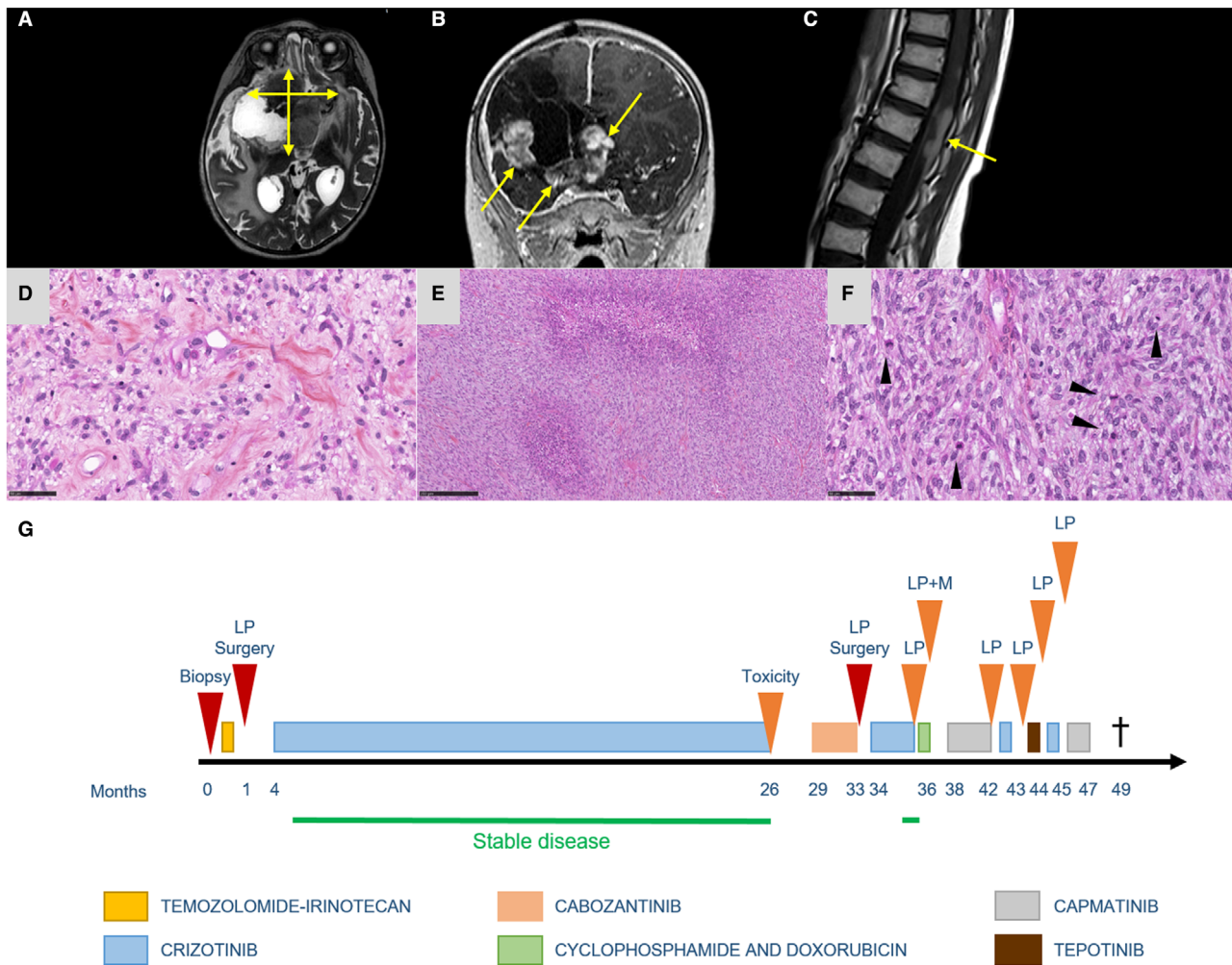


**Figure 5.** Radiological and histopathological features of case 16. (A) Axial T2-weighted image showing a voluminous frontotemporal mass with a solid component and central hyperintense areas suggestive of cystic–necrotic changes and without peritumoral oedema. (B) Axial T2-weighted coronal contrast-enhanced T1-weighted MR image showing a local relapse with enhancing nodules (arrows). (C) Sagittal contrast-enhanced T1-weighted image of the spinal cord showing a spinal metastasis at the level of the medullary cone (arrowhead). (D) Histopathology of the primary tumour showing a low cellular proliferation composed of spindle cells without atypia (HPS). (E) Histopathology of the recurrent tumour showing a high cellular proliferation with frequent areas of necrosis (HPS). (F) The tumour was composed of spindle cells with marked atypia and several mitoses (arrowheads) (HPS). (G) Time-line of the tumour progression and treatment choices as shown (LP, local progression; M, metastases). Scale bars represent 250  $\mu$ m (E) and 50  $\mu$ m (D,F). HPS, haematoxylin phloxin saffron.

limitations of molecular classification that may occasionally further complicate the matter rather than solving it. Additional series are needed to characterise in detail the histomolecular landscape of infantile mesenchymal tumours with *NTRK* fusions. In doubtful cases, perivascular collagen rings is a common feature of these tumours,<sup>16</sup> reminiscent of a *NTRK*-fusion in this morphological setting. Additionally, the presence of a *CDKN2A* deletion also seems common in SCN–*NTRK*, as 9p deletions were previously found in 33% of cases (two of six) in a precedent series.<sup>52</sup> The DNA-methylation profiling correlates more with the cell origin than the tumours' genotype, as was evidenced in

CNS tumours with, for example, tumours sharing MAPK alterations or *ROS1* fusions, and were clearly distinct by epigenetic profiles.<sup>28,53</sup> The two current CNS cases were clearly distinct from infantile hemispheric gliomas sharing *NTRK* fusions. Our isolated case with *MET* fusion clustered among *NTRK*-fused tumours, which may suggest the representation of a genetic variant of the same entity or may emerge later with additional cases as a distinct entity. *TFG::MET* fusion has been previously described in two cases of the soft tissue and the retroperitoneum presenting similar clinical (infants) and histopathological features (spindle cell tumours infiltrating the surrounding tissue



with a high mitotic index for one of them).<sup>21,22</sup> Further studies are needed to confirm that other kinase fusions (*ALK*, *BRAF*, *RAF1*, *ROS1*) are part of the same MC of SCN–NTRK. In the CNS, SCN–NTRK is probably underdiagnosed, and further cases of CNS SCN–NTRK are needed to confirm or not their place in the next WHO Classification of CNS tumours. The outcome of extra-CNS SCN–NTRK seems to be favourable, with a median follow-up of 24 months (ranging from 1 month to 54 years).<sup>5,6,8–13,15,16,18,20,21,25</sup> Recurrences are relatively frequent (35% of cases) and mostly local,<sup>5,13,16,17,22,25</sup> but distant metastases have been reported.<sup>16,17,22</sup> However, only 5% of patients<sup>16,20</sup> die from their disease (median overall survival of 24 months). As illustrated here, targeted therapy (with crizotinib or entrectinib) may be an interesting alternative therapeutic option (for patients with unresectable or recurring tumours).<sup>8,25</sup>

In summary, our study confirms that SCN–NTRK have a common myofibroblastic differentiation throughout the many affected organs and represent a new MC distinct from their differential histomolecular diagnoses, including IFS. Further series are needed to confirm these data and suggest a consensual nosology.

## Acknowledgements

The authors are grateful to the laboratory technicians from GHU Paris Neurosciences, Hospital Sainte-Anne and Institut Bergonie (Bordeaux), for their assistance and the clinicians and pathologists who provided material and clinical follow-up. FLL's research is supported by grants from the Fondation Bergonie, the SIRIC Bordeaux Brio and the charity 'Au fil d'Oriane'. ATE's research is supported by grants from the Fondation 'Liv et Lumière'. AT-E, MD JB, MLeQ, DB, PV and FLeL contributed equally to this work.

## Conflicts of interest

The authors declare that they have no conflicts of interest directly related to the topic of this article.

## References

- Uguen A, Csanyi-Bastien M, Sabourin J-C, Penault-Llorca F, Adam J. How to test for NTRK gene fusions: a practical approach for pathologists. *Ann. Pathol.* 2021; **41**: 387–398.
- Antonescu CR, Suurmeijer AJH, Zhang L et al. Molecular characterization of inflammatory myofibroblastic tumors with frequent *ALK* and *ROS1* gene fusions and rare novel *RET* rearrangement. *Am. J. Surg. Pathol.* 2015; **39**: 957–967.
- Bourgeois JM, Knezevich SR, Mathers JA, Sorensen PHB. Molecular detection of the *ETV6-NTRK3* gene fusion differentiates congenital fibrosarcoma from other childhood spindle cell tumors. *Am. J. Surg. Pathol.* 2000; **24**: 937–946.
- Kallen ME, Hornick JL. The 2020 WHO classification: what's new in soft tissue tumor pathology? *Am. J. Surg. Pathol.* 2021; **45**: e1–e23.
- Agaram NP, Zhang L, Sung Y-S et al. Recurrent *NTRK1* gene fusions define a novel subset of locally aggressive Lipofibromatosis-like neural tumors. *Am. J. Surg. Pathol.* 2016; **40**: 1407–1416.
- Bartenstein DW, Coe TM, Gordon SC et al. Lipofibromatosis-like neural tumor: case report of a unique infantile presentation. *JAAD Case Rep.* 2018; **4**: 185–188.
- Brčić I, Godschachner TM, Bergovec M et al. Broadening the spectrum of NTRK rearranged mesenchymal tumors and usefulness of pan-TRK immunohistochemistry for identification of NTRK fusions. *Mod. Pathol.* 2021; **34**: 396–407.
- Dupuis M, Shen Y, Curcio C et al. Successful treatment of lipofibromatosis-like neural tumor of the lumbar spine with an NTRK-fusion inhibitor. *Clin. Sarcoma Res.* 2020; **10**: 14.
- Haller F, Knopf J, Ackermann A et al. Paediatric and adult soft tissue sarcomas with *NTRK1* gene fusions: a subset of spindle cell sarcomas unified by a prominent myopericytic/haemangiopericytic pattern. *J. Pathol.* 2016; **238**: 700–710.
- Higaki-Mori H, Hisaoka M, Yoshida Y, Ehara Y, Shindo M, Yamamoto O. Infantile lipofibromatosis-like neural tumour investigated by a fusion gene detection assay. *Acta Derm. Venereol.* 2020; **100**: adv00180.
- Kang J, Park JW, Won J-K et al. Clinicopathological findings of pediatric NTRK fusion mesenchymal tumors. *Diagn. Pathol.* 2020; **15**: 114.
- Kohsaka S, Saito T, Akaike K et al. Pediatric soft tissue tumor of the upper arm with *LMNA-NTRK1* fusion. *Hum. Pathol.* 2018; **72**: 167–173.
- Lao IW, Sun M, Zhao M, Yu L, Wang J. Lipofibromatosis-like neural tumour: a clinicopathological study of ten additional cases of an emerging novel entity. *Pathology* 2018; **50**: 519–523.
- Malik F, Santiago T, Newman S, McCarville B, Pappo AS, Clay MR. An addition to the evolving spectrum of lipofibromatosis and lipofibromatosis-like neural tumor: molecular findings in an unusual phenotype aid in accurate classification. *Pathol. Res. Pract.* 2020; **216**: 152942.
- Panse G, Reisenbichler E, Snuderl M, Wang WL, Laskin W, Jour G. *LMNA-NTRK1* rearranged mesenchymal tumor (lipofibromatosis-like neural tumor) mimicking pigmented dermatofibrosarcoma protuberans. *J. Cutan. Pathol.* 2021; **48**: 290–294.
- Suurmeijer AJH, Dickson BC, Swanson D et al. A novel group of spindle cell tumors defined by *S100* and *CD34* co-expression shows recurrent fusions involving *RAF1*, *BRAF*, and *NTRK1/2* genes. *Genes Chromosomes Cancer* 2018; **57**: 611–621.
- Davis JL, Lockwood CM, Albert CM, Tsuchiya K, Hawkins DS, Rudzinski ER. Infantile NTRK-associated mesenchymal tumors. *Pediatr. Dev. Pathol.* 2018; **21**: 68–78.
- Abs D, Landman S, Osio A, Lepesant P, Schneider P, Obadia D, Moguelet P, Farges C, Poirot B, Lehmann-Che J, Lebbé C. Spindle cell tumor with *CD34* and *S100* co-expression and distinctive stromal and perivascular hyalinization showing *EML4-ALK* fusion. *J. Cutan. Pathol.* 2020;**48**(7):896-901.
- Al-Ibraheemi A, Folpe AL, Perez-Atayde AR et al. Aberrant receptor tyrosine kinase signaling in lipofibromatosis: a clinicopathological and molecular genetic study of 20 cases. *Mod. Pathol.* 2019; **32**: 423–434.

20. Antonescu CR, Dickson BC, Swanson D *et al.* Spindle cell tumors with RET gene fusions exhibit a morphologic Spectrum akin to tumors with NTRK gene fusions. *Am. J. Surg. Pathol.* 2019; **43**: 1384–1391.
21. Flucke U, van Noesel MM, Wijnen M *et al.* TFG-MET fusion in an infantile spindle cell sarcoma with neural features. *Genes Chromosomes Cancer* 2017; **56**: 663–667.
22. Kao Y-C, Suurmeijer AJH, Argani P *et al.* Soft tissue tumors characterized by a wide spectrum of kinase fusions share a lipofibromatosis-like neural tumor pattern. *Genes Chromosomes Cancer* 2020; **59**: 575–583.
23. Lopez-Nunez O, Surrey LF, Alaggio R, Fritchie KJ, John I. Novel PPP1CB-ALK fusion in spindle cell tumor defined by S100 and CD34 coexpression and distinctive stromal and perivascular hyalinization. *Genes Chromosomes Cancer* 2020; **59**: 495–499.
24. Paton DJW, Wong D, Amanuel B, Cheah K, Ardakani NM. S100/CD34-positive spindle cell mesenchymal neoplasm harboring KIAA1549-BRAF fusion. *Am. J. Dermatopathol.* 2021; **43**: 217–220.
25. Sheng S-J, Li J-M, Zou Y-F *et al.* A low-grade malignant soft tissue tumor with S100 and CD34 co-expression showing novel CDC42SE2-BRAF fusion with distinct features. *Genes Chromosomes Cancer* 2020; **59**: 595–600.
26. Pfister SM, Reyes-Múgica M, Chan JKC *et al.* A summary of the inaugural WHO classification of pediatric tumors: transitioning from the optical into the molecular era. *Cancer Discov.* 2022; **12**: 331–355.
27. Anderson WJ, Doyle LA. Updates from the 2020 World Health Organization classification of soft tissue and bone Tumours. *Histopathology* 2021; **78**: 644–657.
28. Capper D, Jones DTW, Sill M *et al.* DNA methylation-based classification of central nervous system tumours. *Nature* 2018; **555**: 469–474.
29. Sturm D, Orr BA, Toprak UH *et al.* New brain tumor entities emerge from molecular classification of CNS-PNETs. *Cell* 2016; **164**: 1060–1072.
30. Louis DN, Perry A, Wesseling P *et al.* The 2021 WHO classification of tumors of the central nervous system: a summary. *Neuro Oncol.* 2021; **23**(8): 1231–1251.
31. Hovestadt V, Jones DTW, Picelli S *et al.* Decoding the regulatory landscape of medulloblastoma using DNA methylation sequencing. *Nature* 2014; **510**: 537–541.
32. Zhu T, Liu J, Beck S *et al.* A pan-tissue DNA methylation atlas enables in silico decomposition of human tissue methylomes at cell-type resolution. *Nat. Methods* 2022; **19**: 296–306.
33. Koelsche C, Schrimpf D, Stichel D *et al.* Sarcoma classification by DNA methylation profiling. *Nat. Commun.* 2021; **12**: 498.
34. Perret R, Michal M, Carr RA *et al.* Superficial CD34-positive fibroblastic tumor and PRDM10-rearranged soft tissue tumor are overlapping entities: a comprehensive study of 20 cases. *Histopathology* 2021; **79**: 810–825.
35. Anders S, Pyl PT, Huber W. HTSeq—a python framework to work with high-throughput sequencing data. *Bioinforma. Oxf. Engl.* 2015; **31**: 166–169.
36. Pilson D, Decker KL. A language and environment for statistical computing. *Ecology* 2002; **83**: 3097–3107.
37. Law CW, Chen Y, Shi W, Smyth GK. Voom: precision weights unlock linear model analysis tools for RNA-seq read counts. *Genome Biol.* 2014; **15**: R29.
38. Wilkerson MD, Hayes DN. ConsensusClusterPlus: a class discovery tool with confidence assessments and item tracking. *Bioinformatics* 2010; **26**: 1572–1573.
39. Crumbach L, Descotes F, Bringuier P-P *et al.* Lipofibromatosis-like neural tumor: a case report and review of the literature. *Am. J. Dermatopathol.* 2020; **42**: 881–884.
40. Lyskjaer I, De Noon S, Tirabosco R *et al.* DNA methylation-based profiling of bone and soft tissue tumours: a validation study of the 'DKFZ sarcoma classifier'. *J. Pathol. Clin. Res.* 2021; **7**: 350–360.
41. Eyden B. Electron microscopy in the study of myofibroblastic lesions. *Semin. Diagn. Pathol.* 2003; **20**: 13–24.
42. Eyden B, Banerjee SS, Shenjere P, Fisher C. The myofibroblast and its tumours. *J. Clin. Pathol.* 2009; **62**: 236–249.
43. Mariño-Enríquez A, Wang W-L, Roy A *et al.* Epithelioid inflammatory myofibroblastic sarcoma: an aggressive intra-abdominal variant of inflammatory myofibroblastic tumor with nuclear membrane or perinuclear ALK. *Am. J. Surg. Pathol.* 2011; **35**: 135–144.
44. Bennett JA, Nardi V, Rouzbahman M, Morales-Oyarvide V, Nielsen GP, Oliva E. Inflammatory myofibroblastic tumor of the uterus: a clinicopathological, immunohistochemical, and molecular analysis of 13 cases highlighting their broad morphologic spectrum. *Mod. Pathol.* 2017; **30**: 1489–1503.
45. Lopez-Nunez O, John I, Panasiti RN *et al.* Infantile inflammatory myofibroblastic tumors: clinicopathological and molecular characterization of 12 cases. *Mod. Pathol.* 2020; **33**: 576–590.
46. Papke DJ, Al-Ibraheemi A, Fletcher CDM. Plexiform myofibroblastoma: clinicopathologic analysis of 36 cases of a distinctive benign tumor of soft tissue affecting mainly children and young adults. *Am. J. Surg. Pathol.* 2020; **44**: 1469–1478.
47. Mentzel T, Dry S, Katenkamp D, Fletcher CDM. Low-grade myofibroblastic sarcoma: analysis of 18 cases in the spectrum of myofibroblastic tumors. *Am. J. Surg. Pathol.* 1998; **22**: 1228–1238.
48. Huson SM, Staab T, Pereira M *et al.* Infantile fibrosarcoma with TPM3-NTRK1 fusion in a boy with bloom syndrome. *Fam Cancer* 2020; **21**(1): 85–90.
49. Caldwell KJ, De La Cuesta E, Morin C, Pappo A, Helmig S. A newborn with a large NTRK fusion positive infantile fibrosarcoma successfully treated with larotrectinib. *Pediatr. Blood Cancer* 2020; **67**: e28330.
50. Wong V, Pavlick D, Brennan T *et al.* Evaluation of a congenital infantile Fibrosarcoma by comprehensive genomic profiling reveals an LMNA-NTRK1 gene fusion responsive to Crizotinib. *J. Natl. Cancer Inst.* 2016; **108**: djv307.
51. Mahajan P, Casanova M, Ferrari A, Fordham A, Trahair T, Venkatramani R. Inflammatory myofibroblastic tumor: molecular landscape, targeted therapeutics, and remaining challenges. *Curr. Probl. Cancer* 2021; **45**: 100768.
52. Vargas AC, Ardakani NM, Wong DD *et al.* Chromosomal imbalances detected in NTRK-rearranged sarcomas by the use of comparative genomic hybridisation. *Histopathology* 2021; **78**: 932–942.
53. Sievers P, Stichel D, Sill M *et al.* GOPC:ROS1 and other ROS1 fusions represent a rare but recurrent drug target in a variety of glioma types. *Acta Neuropathol.* 2021; **142**: 1065–1069.

## Supporting Information

Additional Supporting Information may be found in the online version of this article:

**Table S1.** Materials and methods used in this work.